THE JOURNAL OF PHYSICAL CHEMISTRY C

Article

pubs.acs.org/JPCC

pH-Dependent Photocorrosion of GaAs/AlGaAs Quantum Well Microstructures

Hemant Sharma, Khalid Moumanis, and Jan J. Dubowski*

Laboratory for Quantum Semiconductors and Photon-Based BioNanotechnology, Interdisciplinary Institute for Technological Innovation (3IT), CNRS UMI-3463, Department of Electrical and Computer Engineering, Université de Sherbrooke, 2500 boul. de l'Université, Sherbrooke, Québec J1K 2R1, Canada

Supporting Information

ABSTRACT: Semiconductor microstructures comprising stacks of GaAs/AlGaAs layers have found attractive applications for photocorrosion-based detection of electrically charged molecules immobilized in the vicinity of their surfaces. We have investigated sensitivity of the photocorrosion of GaAs/AlGaAs microstructures with a stack of 30 GaAs quantum well (QW) layers to pH of aqueous solutions ranging between 2.2 and 11.2. The effect was studied by measuring QW emission for bare and (3-mercaptopropyl)-trimethoxysilane (MPTMS) coated microstructures. It has been determined that in highly both acidic (pH 2.2) and alkaline (pH 11.2) solutions the uncoated microstructures photocorrode at relatively high rates (~0.83 nm/min), while in moderate pH (7−9) solutions the photocorrosion proceeds at rates reduced to ~0.33 nm/min, suggesting that some oxides accumulate on the *in situ* revealed surfaces of GaAs and $Al_{0.35}Ga_{0.65}As$. The photocorrosion at a moderate-to-high pH 10.2 revealed the formation of a series of well-defined PL maxima each time the photocorrosion front passes from the GaAs to the $Al_{0.35}Ga_{0.65}As$ surface. For MPTMS functionalized samples, a series of similar origin, well-defined PL maxima have been observed in a more alkaline solution characterized by pH of 11.2. A delayed position of the first PL maximum illustrates the passivation function of the MPTMS layer, although its depolymerization is observed in a highly alkaline environment.

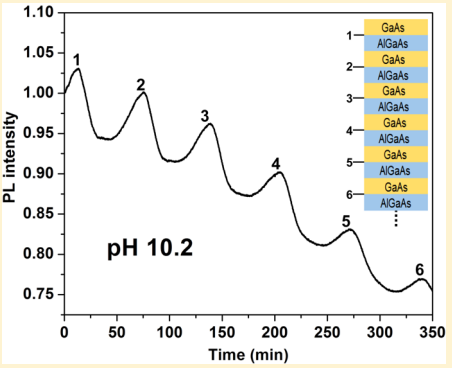

1. INTRODUCTION

Optoelectronic properties of III−V semiconductors have earned these materials a leading role in the development of semiconductor lasers, modulators, detectors, solar cells, and some other devices.[1,2] A great number of these devices is based on quantum well (QW) GaAs/AlGaAs microstructures.[3,4] The performance of devices based on these microstructures is strongly related to both the chemical and the electronic stability of GaAs, a material of choice for capping typical GaAs/AlGaAs QWs. A strong reactivity of GaAs to water leads to formation of Ga and As oxides,[5−8] and makes this material unstable in an atmospheric environment. Furthermore, it has been observed that the products of GaAs oxidation, such as As-oxides, dissolve relatively easily in aqueous environments,[9,10] while Ga-oxides are more stable, especially in solutions with moderate pH.[11]

Numerous methods have been investigated to passivate GaAs chemically and electronically using inorganic sulfides,[12,13] organic thiols and sulfides,[14,15] and self-assembled monolayers (SAMs) of thiols.[16,17] Among a variety of oxides investigated for passivation of GaAs, Ga_2O_3 is of a particular interest due to its ability to reduce the density of surface states and decrease the surface recombination velocity of minority carriers (holes in n-type GaAs), which leads to an increased intensity of the PL signal emitted by this material.[11,18,19] Deposition of Ga_2O_3 thin films on GaAs has been investigated by electron-beam evaporation[18] and molecular beam epitaxy.[20] It also could be formed on the surface of GaAs through the so-called photowashing effect on samples immersed in water and excited with the above bandgap radiation.[21,22]

The stability of an amorphous or polycrystalline Ga_2O_3 layer on GaAs depends on the chemistry of a surrounding environment, including its pH, influencing the rate of oxide formation and photoetching.[6] In the case of oxide semiconductors, the oxide surface states react with H^+ or OH^- ions and affect the pH-dependent flatband potential changing at 60 mV/pH.[23] Based on this effect, some oxide semiconductors have been designed as pH sensors.[24] Moreover, organic layer coated semiconductors have shown a sensitivity to pH.[25] For example, n-type GaAs passivated against corrosion with a thick layer of methoxysilane (3-mercaptopropyl)-trimethoxysilane (MPTMS) shows change in source-drain current against pH of the solution.[26] Thus, while the stability and sensitivity of electronically driven semiconductor-based devices could depend on pH of a surrounding medium, the stability of optically driven devices becomes a critical issue due to the potential pH-dependent photocorrosion of such devices.[27]

In the field of biosensors, pH plays a crucial role in determining the appropriate response, as well as the lifetime of

Received: September 1, 2016
Revised: October 21, 2016
Published: October 26, 2016

DOI: 10.1021/acs.jpcc.6b08844
J. Phys. Chem. C 2016, 120, 26129−26137

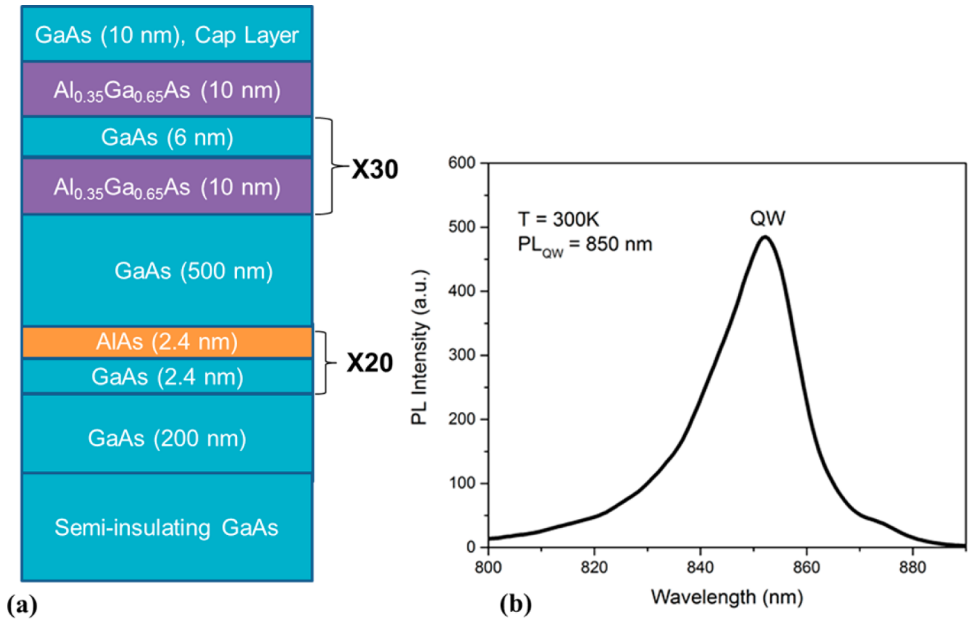

Figure 1. Schematic cross section of the 30-GaAs-QW microstructure investigated in the photocorrosion experiments (a), and 532 nm excited room temperature PL of the microstructure dominated by the 850 nm emission from 6 nm thick GaAs QWs (b).

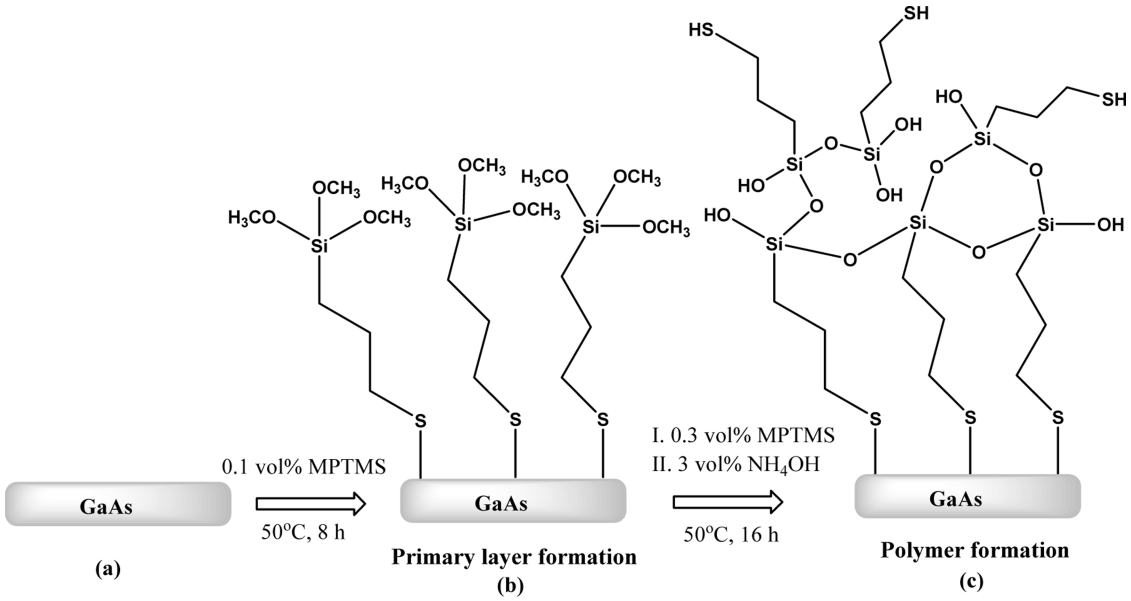

Figure 2. Schematic representation of MPTMS coating on the surface of GaAs: (a) cleaned and etched GaAs sample, (b) primary layer formation, and (c) polymer formation.

a sensor. Most biosensor studies are performed in neutral pH conditions; however, several physiological processes require extreme acidic or alkaline conditions.[28−30] Hence, it is highly relevant to examine the effect of pH on photocorrosion of optically based biosensors, such as GaAs/AlGaAs microstructures investigated for biosensing applications.[31−34] In this study, we employed microstructures consisting of a stack of GaAs/AlGaAs QWs grown on GaAs(001) substrate, and we have investigated mechanisms of pH-dependent oxide formation that drives photocorrosion of these microstructures.

2. EXPERIMENTAL SECTION

2.1. Semiconductor Samples. Samples of GaAs/AlGaAs microstructures investigated in this work (Wafer 10−423, acquired from Azastra Inc., Ottawa, Canada) consist of 30 pairs of GaAs/$Al_{0.35}Ga_{0.65}As$ layers grown on an undoped 500 nm thick GaAs epi-layer deposited on a semi-insulating GaAs(001) substrate. The microstructure is finished with a 10 nm thick $Al_{0.35}Ga_{0.65}As$ barrier and capped with a 10 nm thick GaAs layer. A cross section of the microstructure is shown in Figure 1a. A 200 nm thick GaAs buffer and a 20-pair AlAs/GaAs stack were employed to achieve high structural quality of the whole epitaxial microstructure. Figure 1b shows room temperature photoluminescence (PL) from this microstructure recorded with a commercial PL mapper (Philips PLM-150) equipped with a constant power 532 nm excitation source and an IR array of InGaAs detectors. It can be seen that the PL spectrum is

DOI: 10.1021/acs.jpcc.6b08844
J. Phys. Chem. C 2016, 120, 26129−26137

dominated by an 850 nm emission that originates from 6 nm thick GaAs QWs.

2.2. Material and Reagents. All studies were performed at room temperature (25 °C). High purity (95%) (3-mercaptopropyl)-trimethoxysilane (MPTMS) was purchased from Sigma-Aldrich (Oakville, Canada). OptiClear, acetone, isopropyl alcohol (IPA), and anhydrous ethanol was obtained from National Diagnostics (Mississauga, Canada), ACP Chemicals Inc. (Montréal, Canada), Fisher Scientific (Ottawa, Canada), and Commercial Alcohols, Inc. (Brampton, Canada), respectively. Ammonium hydroxide (28%) was purchased from Anachemia (Richmond, Canada). High-purity (99.999%) compressed nitrogen gas was purchased from Praxair, Canada. Water was deionized to 18.2 MΩ resistance (DI water) with a Millipore purification custom system built by Culligan (Québec, Canada).

2.3. GaAs/AlGaAs QW Microstructures with MPTMS Coated Surface. Chips of 2 mm × 2 mm dimensions were diced from the GaAs/AlGaAs wafer whose surface was protected by spin-coated photoresist. The chips were sequentially cleaned in OptiClear, acetone, isopropanol, acetone, and ethanol through 10 min sonication in each solvent. Next, they were etched in 2% hydrofluoric acid (HF) for 5 s, rinsed in deionized water (1 s), etched in ammonium hydroxide (NH_4OH 28%) for 30 s, and rinsed in DI water (1 s). This etching procedure removes native oxides such as Ga_2O_3, As_2O_5, and As_2O_3.[15] After etching, the chips were rinsed in degassed anhydrous ethanol, followed by drying with a flow of high-purity compressed nitrogen gas, and immediately transferred into 0.1 vol % MPTMS alcoholic solution. A small vessel with the 0.1 vol % MPTMS alcoholic solution containing chips was placed in an oil bath at 50 °C for 8 h. This procedure is expected to form a uniform primary layer on the surface of GaAs through the exposure to thiol end groups.[15] This step was followed by polymerization of MPTMS achieved by increasing the MPTMS concentration to 0.3 vol % in ethanol and adding NH_4OH 28% (3 vol %) as schematically illustrated in Figure 2. The $-OCH_3$ group of MPTMS converts into −OH, which results in an intermolecular condensation reaction between two −OH groups and forming Si−O−Si bond.[15] The solution containing chips was allowed to heat at 50 °C for another 16 h to complete the polymerization. Finally, the chips were rinsed in degassed ethanol and dried under flow of nitrogen.

The response of bare and MPTMS coated samples to different pH aqueous environments was investigated for acidic and alkaline solutions comprising different concentrations of HCl and NaOH to cover the pH range from 2.1 to 11.2.

2.4. Photoluminescence Monitored Photocorrosion. Temporal PL plots were recorded using a custom designed Quantum Semiconductor Photonic Biosensor (QSPB) reader.[34] The samples were irradiated with 2 s pulses in every 8 s period using a homogenized beam of an LED operating at 660 nm and delivering power of 9 mW/cm^2 to the sample surface. A long-pass optical filter with the transmission wavelength threshold at near 820 nm was used to collect integrated PL signals recorded with a CCD camera of the QSPB reader.

2.5. Surface Characterization. *2.5.1. Fourier-Transform Infrared (FTIR) Analysis.* The spectra were recorded in a transmission mode using a Bruker Optics Hyperion 2000 FTIR system. The spectral resolution was 4 cm^{-1}, and each spectrum was averaged over 512 scans. All FTIR studies were performed in a vacuum chamber of the Vertex 70v spectrometer. The spectra were recorded by a liquid N_2 cooled HgCdTe (MCT) broadband detector. A sample cleaned by a series of organic solvents (OptiClear, acetone, isopropanol, acetone, and ethanol; sonication 10 min each) followed by etching (2% HF and 28% NH_4OH) was used as reference.

2.5.2. Atomic Force Microscopy (AFM) Analysis. The measurements were performed using a Nanoscope III microscope (Digital Instruments, Inc.) operating in a tapping mode. All AFM images were recorded at room temperature and in an atmospheric air environment. The root-mean-square surface roughness (σ_{RMS}) was determined based on scans collected from 5 μm × 5 μm surface areas of the investigated samples averaged over two independent areas of each sample. The reference sample was prepared as described in section 2.5.1.

2.5.3. X-ray Photoelectron Spectroscopy (XPS). To collect XPS spectra, we employed an Axis Ultra DLD (Kratos Analytical Ltd.; UK) system equipped with a monochromatic Al Kα source (1486.6 eV). The measurements were carried out in a vacuum chamber (<10^{-9} Torr). The surface survey scans and high-resolution scans were measured using analyzers with pass energy of 160 and 20 eV, respectively. The data were collected for a takeoff angle of 60° with respect to the surface normal. Peak fitting and quantification analysis were done using the software package CasaXPS.[35] Binding energy scale was calibrated versus adventitious carbon 1s peak at 284.8 eV.

3. RESULTS AND DISCUSSION

The formation of a primary layer and polymerization steps were characterized with FTIR absorption spectroscopy. Figure 3a shows an FTIR spectrum of the MPTMS primary layer on the surface of GaAs. The peaks at 2850, 2925 and 2958 cm^{-1} indicate the position of symmetric CH_2 stretch (ν_s-CH_2), asymmetric CH_2 stretch (ν_a-CH_2), and asymmetric CH_3 stretch (ν_a-CH_3) groups of MPTMS, respectively. Similarly, Si-OCH_3 and Si-CH_2 groups are characterized by peaks at 1077 and 1196 cm^{-1}, respectively, as shown in that figure. The polymerization of MPTMS involved cleavage of Si-OCH_3 bonds and simultaneous formation of Si−O−Si bonds through condensation reaction. This produced a cross-linked three-dimensional structure. The polymerization of the MPTMS layer was confirmed by the appearance of Si−O−Si bond peaks at 1126, 810, and 531 cm^{-1} corresponding to asymmetric stretching, symmetric stretching/bending, and rocking,[36] respectively, as shown in Figure 3b. Furthermore, absence of CH_3 peak in the spectrum of polymerized structure indicates the cleavage of the Si−OCH_3 bonds, while the broad band around 3250 cm^{-1} indicates the H-bonded silanol groups (Si−OH),[37] as shown in Figure 3b. The peaks at 2923 and 2859 cm^{-1} correspond to symmetric CH_2 stretch (ν_s-CH_2) and asymmetric CH_2 stretch (ν_a-CH_2). It can also be seen that the polymerization step produced some free −SH groups at 2556 cm^{-1}. Figure S1 in Supporting Information provides details of the FTIR spectra for both primary and polymer layers, clearly confirming the formation of a primary layer and its polymerization on the surface of GaAs. To the best of our knowledge, these results provide the first FTIR evidence of MPTMS primary and polymer layers formed on the surface of GaAs.

Figure 4 shows examples of temporal PL plots of bare and MPTMS functionalized GaAs/AlGaAs QW microstructures photocorroding in DI water. The characteristic PL maxima observed for both samples are related to the formation of As- and Ga-oxides and dissolution of the 10 nm thick GaAs cap layer.[33,34]

DOI: 10.1021/acs.jpcc.6b08844
J. Phys. Chem. C 2016, 120, 26129−26137

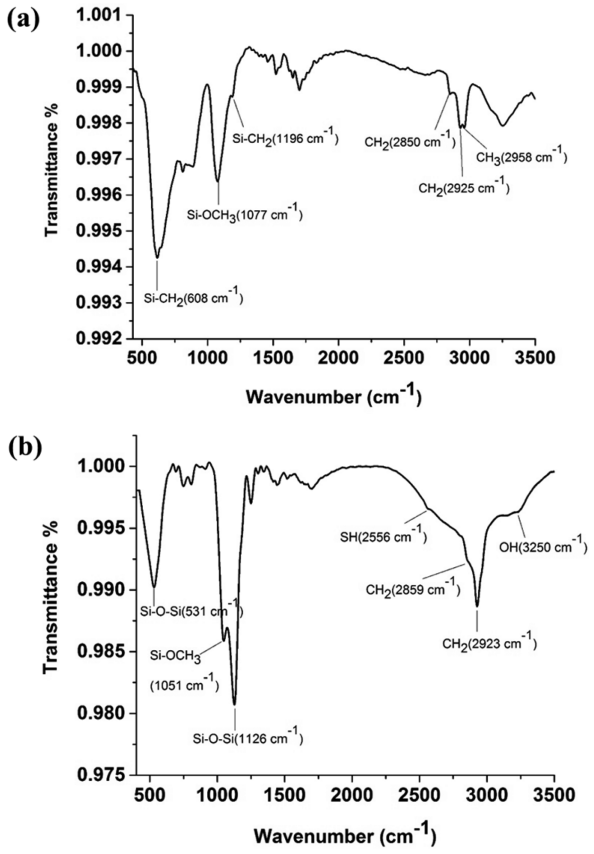

Figure 3. FTIR spectra of MPTMS coated samples after formation of the primary layer (a) and after polymerization of the MPTMS layer (b).

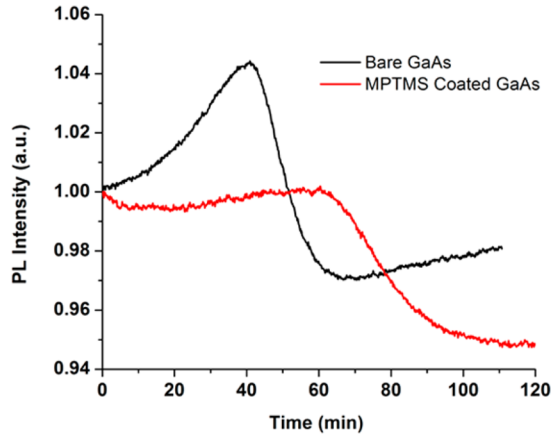

Figure 4. Comparison of temporal QW PL emission at ~850 nm from a bare and MPTMS coated GaAs/AlGaAs microstructure exposed to DI water and pulse-irradiated with a 660 nm LED.

In agreement with the previous reports,[21,38] we observed the enhancement of a PL signal from GaAs immersed in an aqueous environment due to formation of a quasi-stable Ga_2O_3 layer that was induced by the above bandgap excitation. A dissolution of such a layer has been observed, for instance, in early experiments of laser-induced corrosion of GaAs in an aqueous medium of pH ~ 6.6.[39] In our case, as the GaAs/AlGaAs interface is revealed, a drastically increased surface concentration of nonradiative recombination centers, typical of the AlGaAs surface,[40] leads to a significant decay of the PL

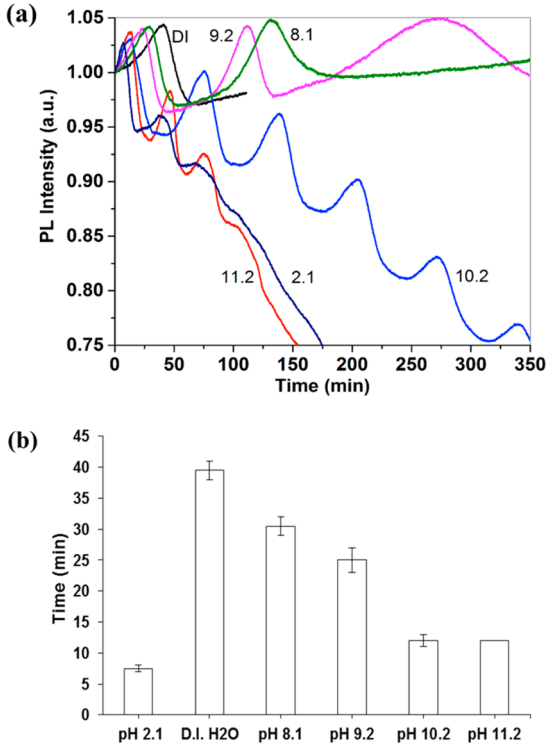

Figure 5. Time-dependent PL plots of bare GaAs/AlGaAs QW microstructures photocorroding in different pH aqueous solutions (a), and a bar graph indicating the occurrence of the first PL maximum (b).

signal and formation of PL maxima observed for both samples.[33,34] It can be seen that the amplitude of a PL maximum from MPTMS coated GaAs is significantly weaker than that of the bare GaAs sample, and its position is delayed by approximately 20 min. This suggests that the MPTMS layer slowed down the photocorrosion of the GaAs/AlGaAs microstructure, and the process of material dissolution followed a mechanism different from that concerning bare GaAs.

Generally, surface passivation of III−V semiconductors with alkanethiol self-assembled monolayers (SAMs) enhances their PL intensity due to the reduced number of surface states and decreased surface recombination velocity (SRV) of electron and holes.[14,17,41−44] The amplitude of alkanethiol SAM enhanced PL depends upon several factors, such as methylene chain length (typically less than 2 nm), wetting characteristic of SAM, and time of thiolation that defines the quality of SAMs. Passivation of GaAs with MPTMS has been investigated as an attractive alternative to alkanethiol SAMs due to the potential of providing enhanced passivation by a significantly thicker polymerized architecture.[45] However, a polymerized cross-linked MPTMS overlayer, approximately 40 nm thick,[15] while offering reduced oxygen permeability, which results in improved stability of the GaAs surface, could also attenuate the PL signal. This behavior seems to be observed in Figure 4, where a reduced-amplitude PL maximum is formed for the MPTMS coated GaAs/AlGaAs microstructure, while a delayed position of this maximum suggests a reduced rate of photocorrosion.

In Figure 5, we present the results of photocorrosion investigated for bare GaAs/AlGaAs QW samples exposed to aqueous solutions with pH between 2.1 and 11.2. Examples of temporal PL plots in Figure 5a indicate formation of maxima, each time a GaAs/AlGaAs interface is revealed by the

DOI: 10.1021/acs.jpcc.6b08844
J. Phys. Chem. C 2016, 120, 26129−26137

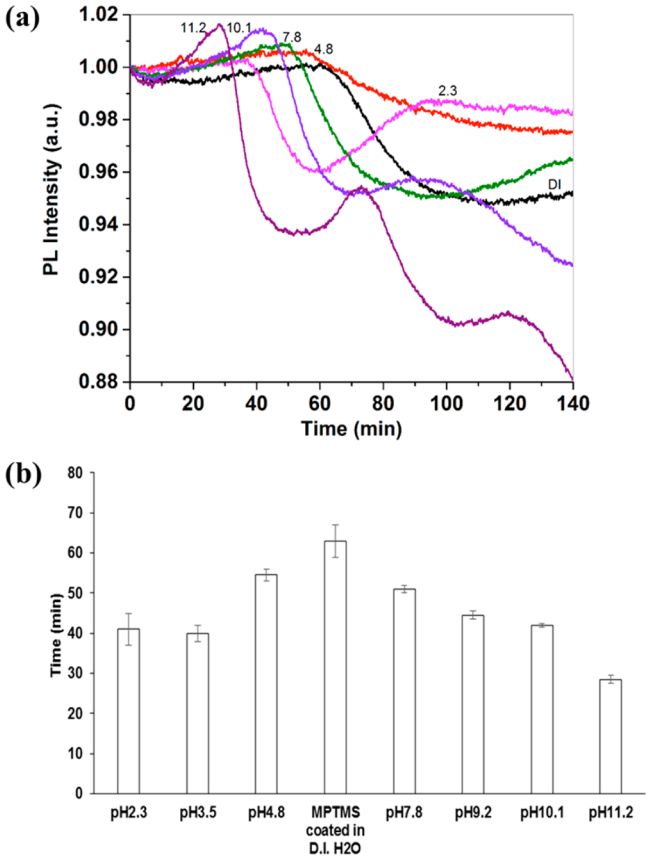

Figure 6. Time-dependent PL plots of MPTMS coated GaAs/AlGaAs microstructures photocorroding in different pH aqueous solutions (for clarity, some plots have been omitted) (a), and a bar graph indicating the occurrence of the first PL maximum in solutions with different pH (b).

photocorrosion process.[46,34] These results allow to identify three distinctively different regions of photocorrosion. At near neutral alkaline environment, $6 < \text{pH} \leq 9.2$, the rate of oxide generation, R_{gen}, is slow but exceeds slightly that of oxide removal, R_{rem}, ($R_{gen} > R_{rem}$). The result is a slowly accumulating layer of oxides on the surface of photocorroding material, making it difficult to observe more than two maxima within a 350 min long experiment. The pH 9.2 plot shows formation of the third maximum with full-width-at-half-maximum significantly larger than those of the first two maxima. This suggests formation of an oxide layer that contributes toward increased screening of the semiconductor−electrolyte reaction and, consequently, slows down the photocorrosion process. At a moderate alkaline environment, pH ≈ 10.2, the rate of oxide generation is also slow, but it nears that of oxide removal ($R_{gen} \approx R_{rem}$). Under these conditions, the photocorroding surface is continuously refreshed with oxides forming at a rate allowing to resolve formation of six independent electrolytic junctions involving 6 nm GaAs QW embedded between 10 nm thick $Al_{0.35}Ga_{0.65}As$ layers. The maxima, equally spaced at 64 min, suggest a steady rate photocorrosion process. In high acidic and high alkaline environments, pH ≈ 2.1 and pH ≈ 11.2, the photocorrosion proceeds at relatively high rates due to high both R_{gen} and R_{rem}. Weakly defined 3−4 maxima are observed in this case on the plots of rapidly decaying PL signals. In Figure 5b, we show a bar graph indicating temporal positions of the first PL maximum revealed in each case and averaged over three independent runs. It can be seen that the most delayed formation of this maximum (slow photocorrosion) occurs at near neutral alkaline conditions, while its rapid formation (fast photocorrosion) is revealed in pH 2.1, 10.2, and 11.2. The advantage of employing microstructures with stacks of QWs is evident in these studies, as by rapidly determining conditions leading to generation of the higher order maxima, it allows to elaborate on the mechanism of photocorrosion.

In the presence of holes (h^+) and H_2O, GaAs undergoes photocorrosion involving production of Ga cations and elemental As atoms:

$$GaAs + 3h^+ + H_2O \rightarrow Ga(III) + As(0) \quad (1)$$

while the elemental As converts into ionic form according to the following equation:

$$As(0) + 3h^+ + H_2O \rightarrow As(III) \quad (2)$$

Ga(III) and As(III) cations are present in different forms of oxides, such as As_2O, AsO, As_2O_3, Ga_2O, GaO, and Ga_2O_3.[47] The solubility of these oxides depends upon pH of a medium. For instance, in an alkaline environment, Ga_2O_3 is insoluble at neutral pH, but it readily converts into soluble gallium hydroxide ion $[Ga(OH)_4]^-$ under strong alkaline conditions:[48]

$$Ga_2O_3 \rightarrow Ga(OH)_4^- \quad (3)$$

Arsenic oxides are also soluble in alkaline solutions, transforming into arsenites. At extremely alkaline conditions (pH 11.2), the rate of oxide dissolution is much higher than the oxidation rate of GaAs and AlGaAs, resulting in a rapid etching of the QW microstructure as illustrated in Figure 5. At near neutral alkaline environment (pH 6−9.2), Ga_2O_3 and As_2O_3 oxides are less soluble and tend to accumulate on the surface of GaAs and AlGaAs semiconductors. This results in weaker photocorrosion, illustrated by the absence of the third maximum at pH 8.1, while a significantly broader maximum related to this feature is observed at pH 9.2. At moderate alkaline condition of pH 10.2, the rates of formation and dissolution of surface oxides are comparable, which results in a constant-rate photocorrosion manifested by formation of equally spaced PL maxima. Under extremely acidic conditions (pH 2.1), Ga_2O_3 converts into soluble gallic ions (Ga^{3+} or $[Ga(H_2O)_6]^{+3}$) that have high solubility in low pH environment.[9] As_2O_3 is less soluble in an acidic medium compared to an alkaline environment;[9] however, it transforms into $AsCl_3$ in the presence of HCl and dissolves easily in an aqueous medium:

$$As_2O_3 + HCl \rightarrow 2AsCl_3 + 3H_2O \quad (4)$$

Thus, at low pH (pH ≈ 2.1), both Ga_2O_3 and As_2O_3 dissolve easily, leaving elemental As(0) on the surface of GaAs and AlGaAs. The higher ratio of Ga/As on GaAs exposed to alkaline medium in comparison to that in acidic medium has been observed with XPS experiments.[27] The elemental As(0) layer is highly porous and not expected to affect the rate of photocorrosion.[27] Therefore, time-dependent PL plots of GaAs/AlGaAs microstructures under extreme acidic or alkaline condition are almost the same (Figure 4a). We note that decay of the PL signal illustrated by the plots at pH 2.1, 10.2, and 11.2 in Figure 5 is consistent with the diminishing number of QWs contributing to the overall PL signal.

DOI: 10.1021/acs.jpcc.6b08844
J. Phys. Chem. C 2016, 120, 26129−26137

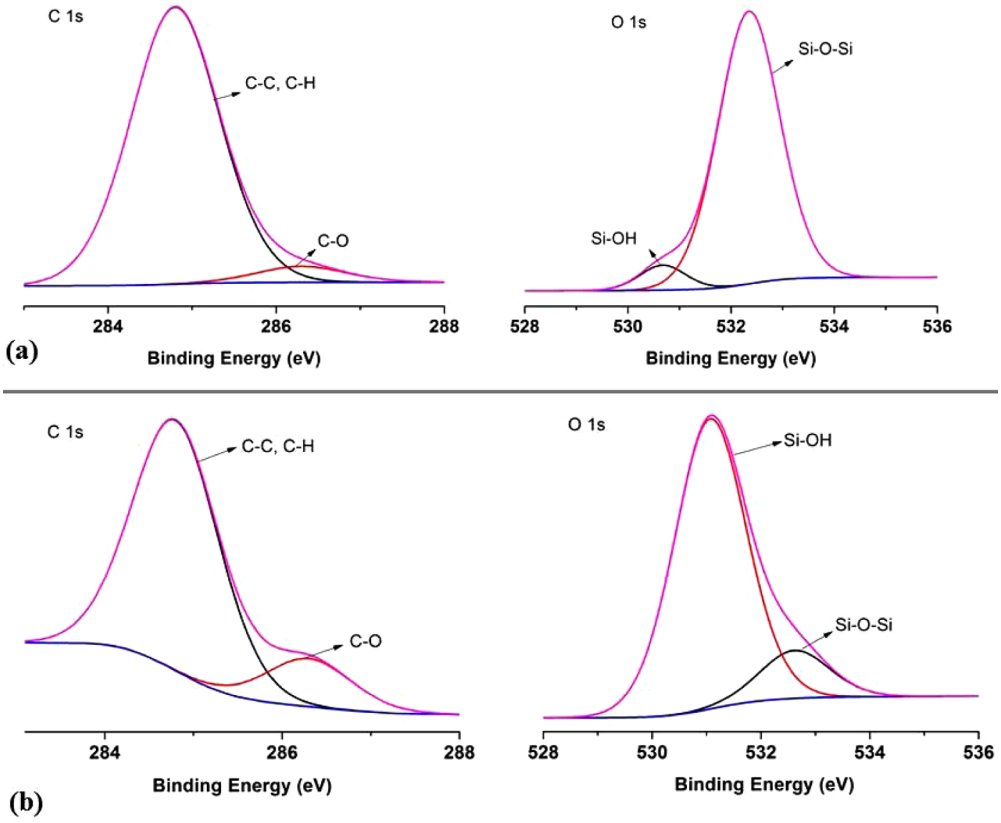

Figure 7. C 1s and O 1s XPS of MPTMS coated samples (a) before and (b) after photocorrosion in alkaline (pH 11.1) medium.

A series of PL plots of MPTMS coated GaAs/AlGaAs samples photocorroding under pH between 2.3 and 11.2 is shown in Figure 6a.

It can be seen that the average intensity of the PL signal observed for low and moderate pH (2.3, 4.8, 7.8, 9.2) decreases at significantly slower rates than that of the signal from the bare samples (see Figure 5). Consistent with this is a delayed position of the first PL maximum that in pH ≈ 2.2 occurs at 41 vs 8 min, while in DI H_2O at 65 vs 40 min, and in pH 9.2 at 44 vs 25 min. Under strongly alkaline conditions of pH 10.1 and 11.2, the average photocorrosion rates appear faster, although they do not exceed those of bare GaAs samples. For instance, the PL of an MPTMS coated sample decreased 12% after a 140 min photocorrosion in pH 11.2, which compares to a 24% decreased PL of a bare sample photocorroding for the same period of time in pH 11.2. Incidentally, the most pronounced series of PL maxima for an MPTMS coated sample is observed for pH 11.2, a more alkaline environment in comparison to that required for achieving a steady rate photocorrosion of bare microstructures. A slowed down photocorrosion in this case is also illustrated by a delayed position of the first maximum that occurs at 28 min in comparison to 12 min that has been observed for a bare sample (Figure 5a). However, comparable positions of the second and third maxima observed for bare at pH 10.2 and MPTMS coated at pH 11.2 samples suggest some loss of protection provided by MPTMS. It appears that this behavior is related to the depolymerization of MPTMS exposed to strong acidic or alkaline environments.[49−51] The formation of siloxane (Si−O−Si) bond is mainly responsible for polymerization of MPTMS, and it undergoes slow hydrolysis under neutral conditions.[49] A water molecule cleavages the siloxane bond and produces silanol:

$$\equiv Si{-}O{-}Si\equiv + H_2O \rightarrow 2\equiv SiOH \quad (5)$$

The addition of acidic or basic solution catalyzed the above reaction, leading to depolymerization with the formation of low molecular weight byproducts. Simultaneously, the process of photocorrosion removed GaAs/AlGaAs heterojunctions one after the other.

To further investigate the mechanism of MPTMS coated and photocorroding GaAs, we carried out XPS measurements of selected samples as a function of the photocorrosion time in an alkaline medium at pH 11.1. The C 1s XPS spectra of as-coated and photocorroded for 140 min samples are presented, respectively, in Figure 7a,b. The quantitative analysis showed that the MPTMS coated sample exhibits 59.3% atomic concentration of carbon. This was reduced to 15.3% after 140 min of photocorrosion in alkaline medium, suggesting that a partially depolymerized MPTMS layer still remains at the surface of a photocorroded microstructure.

The O 1s spectra of the as-fabricated MPTMS layer have been deconvoluted into Si−O−Si and Si−OH that appear at 532.37 and 530.67 eV, respectively.[52] The intensity ratio of (Si−O−Si/Si−OH) peak provides the information about depolymerization that leads to cleavage of Si−O−Si bonds and formation of Si−OH bonds (see Figure S2 in Supporting Information). The decrease in Si−O−Si/Si−OH peaks intensity from 1.36 to 0.82 upon photocorrosion in alkaline medium also indicates the process of depolymerization.

The photocorrosion results for both groups of samples have been corroborated by a study of their surface roughness. Figure 8 shows AFM images of a bare GaAs sample that underwent a 350 min photocorrosion as described in section 2.4 while exposed in pH 2 (Figure 8a) and pH 10 (Figure 8b) solutions. It can be seen that the sample photocorroded in alkaline

DOI: 10.1021/acs.jpcc.6b08844
J. Phys. Chem. C 2016, 120, 26129−26137

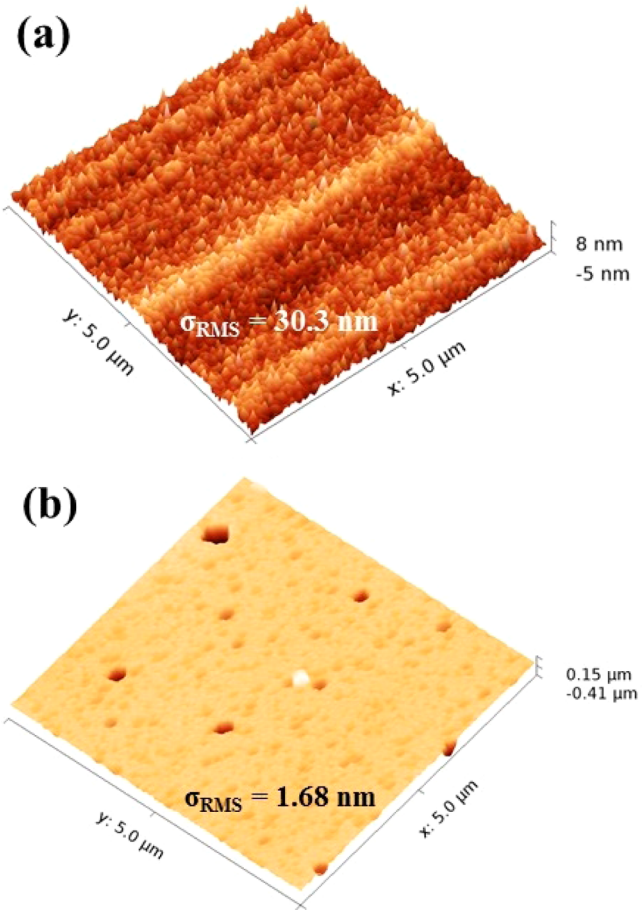

Figure 8. AFM images (5 μm × 5 μm) of bare GaAs after 350 min photocorrosion in pH 2 (a) and pH 10 (b).

Table 1. AFM Images Analysis of MPTMS Coated and Bare Samples

no.	sample	roughness, σ_{RMS} (nm)
1	Reference	1.67 nm
2	MPTMS coated	3.41 nm
3	MPTMS coated, exposed to DI water[a]	4.54 nm
4	MPTMS coated, exposed to pH 2[a]	13.86 nm
5	MPTMS coated, exposed to pH 10[a]	4.46 nm
6	MPTMS coated, exposed to pH 11[a]	3.28 nm
7	Bare, exposed to pH 2[b]	30.3 nm
8	Bare, exposed to pH 10[b]	1.68 nm

[a]Recorded after 140 min irradiation with 2 s pulses in every 8 s period using an LED operating at 660 nm and delivering power of 9 mW/cm^2. [b]Recorded after 350 min irradiation with 2 s pulses in every 8 s period using an LED operating at 660 nm and delivering power of 9 mW/cm^2.

medium (pH 10) is characterized by σ_{RMS} = 1.68 nm, which is practically identical to σ_{RMS} = 1.67 nm observed for the reference sample. This result is consistent with a constant rate of photocorrosion of the GaAs/AlGaAs microstructure as suggested by a related PL plot in Figure 5a. In contrast, the sample photocorroded in acidic medium (pH 2) is characterized by σ_{RMS} of 30.3. As suggested by the results in Figure 5a, at low pH, both Ga- and As-oxides dissolve relatively easily, leaving elemental As(0) on the surface of a photocorroding microstructures. It seems that it is the presence of that As(0) that leads to the formation of an increased roughness surface. The results of a systematic AFM analysis of depolymerized samples, and the effect of pH conditions on σ_{RMS} of MPTMS coated and bare samples is presented in Supporting Information (Figure S3). Table 1 compares σ_{RMS} values for the investigated samples.

These results are consistent with the mechanism of dissolution of GaAs and AlGaAs that proceeds at comparable rates in a basic medium, leading to the development of a smooth surface. The surface roughness of a reference sample increased from σ_{RMS} = 1.67 to 3.42 nm after MPTMS coating, which seems reasonable given the three-dimesional structure of MPTMS.[15] Following the 140 min photocorrosion in deionized water, the surface roughness of such a sample is characterized by σ_{RMS} = 4.54 nm. However, the same time photocorrosion in pH 11 produced the surface with σ_{RMS} = 3.28 nm, while the surface with σ_{RMS} = 13.86 nm has been fabricated in pH 2. The increased roughness of microstructures photocorroding in an acidic environment is most likely related to the precipitation of porous elemental As(0) as well as some depolymerization byproducts.

These results, in addition to demonstrating an innovative application of the PL effect for monitoring pH-dependent photocorrosion of III−V semiconductors, describe an attractive diagnostic tool that could find applications in tuning the operation conditions of photocorrosion-based biosensors.

4. CONCLUSIONS

Effect of pH has been investigated on the photocorrosion of PL emitting bare and MPTMS coated Si-doped GaAs/$Al_{0.35}Ga_{0.65}As$ QW microstructures. The QWs in the microstructures served as markers allowing to study the mechanism of photocorrosion that is dependent on the rate of oxide formation and dissolution. The time-dependent PL plots of photocorroding microstructures revealed maxima corresponding to transition from GaAs−electrolyte to AlGaAs−electrolyte interfaces. It has been determined that the rate of photocorrosion of bare samples is significantly greater in strong acidic and alkaline environments, in agreement with literature data concerning solubility of Ga and As oxides (Ga_2O_3 and As_2O_3). The AFM measurements indicated that the surface roughness (σ_{RMS}) of samples photocorroding in alkaline medium was significantly smoother than those in acidic medium. A time-dependent series of well-resolved PL maxima observed for GaAs/AlGaAs microstructures photocorroding at pH 10.2 suggests that under such conditions the rates of oxide formation and dissolution are relatively slow and comparable. Consequently, we were able to demonstrate a constant rate photocorrosion of a top 100 nm thick GaAs/AlGaAs microstructure. The photocorrosion rates of microstructures immersed in near neutral or moderate pH environments are significantly reduced, primarily due to accumulation of some photocorrosion products at the surface. It seems reasonable that under optimized conditions this process could reveal a significantly greater number of deeply located GaAs QWs. The practical significance of these results is that they demonstrate the feasibility of an innovative metrology method dedicated for cross-sectional profiling of PL emitting multi-heterostructures. The passivation of the GaAs/AlGaAs microstructures with MPTMS leads to a slowed down photocorrosion, consistent with a delayed position of the PL maximum observed as a result of the photocorrosion of a 10 nm thick GaAs cap layer. However, formation of PL maxima related to the photo-

DOI: 10.1021/acs.jpcc.6b08844
J. Phys. Chem. C 2016, 120, 26129−26137

corrosion of deeply located GaAs QWs seemed unaffected by the presence of the MPTMS layer. Our results indicate that depolarization of the MPTMS layer takes place in a strongly alkaline (pH ≈ 11) environment, although partial presence of MPTMS has been observed in such a case, even on the surface of a microstructure photocorroded by 52 nm.

■ ASSOCIATED CONTENT

Supporting Information

The Supporting Information is available free of charge on the ACS Publications website at DOI: 10.1021/acs.jpcc.6b08844.

FTIR spectra of the primary and polymer MPTMS layers, process of MPTMS depolymerization, and AFM images (PDF)

■ AUTHOR INFORMATION

Corresponding Author

*E-mail jan.j.dubowski@usherbrooke.ca. Tel +01-819-821-8000, ext. 62528. Webpage: http://www.dubowski.ca.

Notes

The authors declare no competing financial interest.

■ ACKNOWLEDGMENTS

The research reported in this document was supported by the Canada Research Chair in Quantum Semiconductors Program, and the NSERC Discovery Grant RGPIN-2015-04448. The authors thank Sonia Blais (Centre de caractérisation des matériaux, Université de Sherbrooke) for collecting the XPS results. H.S. acknowledges the Merit Scholarship Program for Foreign Students, Fonds de recherche du Québec - Nature et technologies, for providing a postdoctoral student scholarship.

■ REFERENCES

(1) Brodsky, M. H. Progress in Gallium Arsenide Semiconductors. *Sci. Am.* **1990**, *262*, 68−75.

(2) Kirchner, C.; George, M.; Stein, B.; Parak, W. J.; Gaub, H. E.; Seitz, M. Corrosion Protection and Long-Term Chemical Functionalization of Gallium Arsenide in an Aqueous Environment. *Adv. Funct. Mater.* **2002**, *12*, 266−276.

(3) Bett, A. W.; Dimroth, F.; Stollwerck, G.; Sulima, O. V. III-V Compounds for Solar Cell Applications. *Appl. Phys. A: Mater. Sci. Process.* **1999**, *69*, 119−129.

(4) Yoon, J.; Jo, S.; Chun, I. S.; Jung, I.; Kim, H.-S.; Meitl, M.; Menard, E.; Li, X.; Coleman, J. J.; Paik, U.; et al. GaAs Photovoltaics and Optoelectronics Using Releasable Multilayer Epitaxial Assemblies. *Nature* **2010**, *465*, 329−333.

(5) Bard, A. J.; Wrighton, M. S. Thermodynamic Potential for the Anodic Dissolution of n-Type Semiconductors: A Crucial Factor Controlling Durability and Efficiency in Photoelectrochemical Cells and an Important Criterion in the Selection of New Electrode/Electrolyte Systems. *J. Electrochem. Soc.* **1977**, *124*, 1706−1710.

(6) Lee, H.-Y. Growth of GaAs Oxide Layer Using Photoelectrochemical Method. *J. Electrochem. Soc.* **2008**, *155*, G141−G144.

(7) Ye, P. D.; Wilk, G. D.; Tois, E. E.; Wang, J. J. Formation and Characterization of Nanometer Scale Metal-Oxide-Semiconductor Structures on GaAs Using Low-Temperature Atomic Layer Deposition. *Appl. Phys. Lett.* **2005**, *87*, 013501.

(8) Huang, Y. L.; Chang, P.; Yang, Z. K.; Lee, Y. J.; Lee, H. Y.; Liu, H. J.; Kwo, J.; Mannaerts, J. P.; Hong, M. Thermodynamic Stability of $Ga_2O_3(Gd_2O_3)$/GaAs Interface. *Appl. Phys. Lett.* **2005**, *86*, 191905.

(9) Wang, H. H.; Wu, J. Y.; Wang, Y. H.; Houng, M. P. Effects of pH Values on the Kinetics of Liquid-Phase Chemical-Enhanced Oxidation of GaAs. *J. Electrochem. Soc.* **1999**, *146*, 2328−2332.

(10) Liliental-Weber, Z.; Wilmsen, C. W.; Geib, K. M.; Kirchner, P. D.; Baker, J. M.; Woodall, J. M. Structure and Chemical Composition of Water-Grown Oxides of GaAs. *J. Appl. Phys.* **1990**, *67*, 1863−1867.

(11) Passlack, M.; Hong, M.; Schubert, E. F.; Kwo, J. R.; Mannaerts, J. P.; Chu, S. N. G.; Moriya, N.; Thiel, F. A. In Situ Fabricated Ga_2O_3−GaAs Structures with Low Interface Recombination Velocity. *Appl. Phys. Lett.* **1995**, *66*, 625−627.

(12) Bessolov, V. N.; Lebedev, M. V.; Ivankov, A. F.; Bauhofer, W.; Zahn, D. R. T. Electronic Properties of GaAs(100) Surface Passivated in Alcoholic Sulfide Solutions. *Appl. Surf. Sci.* **1998**, *133*, 17−22.

(13) Konenkova, E. V. Modification of GaAs(100) and GaN(0001) Surfaces by Treatment in Alcoholic Sulfide Solutions. *Vacuum* **2002**, *67*, 43−52.

(14) Lunt, S. R.; Ryba, G. N.; Santangelo, P. G.; Lewis, N. S. Chemical Studies of the Passivation of GaAs Surface Recombination Using Sulfides and Thiols. *J. Appl. Phys.* **1991**, *70*, 7449−7467.

(15) Tkachev, M.; Anand-Kumar, T.; Bitler, A.; Guliamov, R.; Naaman, R. Enabling Long-Term Operation of GaAs -Based Sensors in Aqueous Solutions. *Engineering* **2013**, *5*, 1−12.

(16) Baum, T.; Ye, S.; Uosaki, K. Formation of Self-Assembled Monolayers of Alkanethiols on GaAs Surface with in Situ Surface Activation by Ammonium Hydroxide. *Langmuir* **1999**, *15*, 8577−8579.

(17) Arudra, P.; Marshall, G. M.; Liu, N.; Dubowski, J. J. Enhanced Photonic Stability of GaAs in Aqueous Electrolyte Using Alkanethiol Self-Assembled Monolayers and Postprocessing with Ammonium Sulfide. *J. Phys. Chem. C* **2012**, *116*, 2891−2895.

(18) Passlack, M.; Schubert, E. F.; Hobson, W. S.; Hong, M.; Moriya, N.; Chu, S. N. G.; Konstadinidis, K.; Mannaerts, J. P.; Schnoes, M. L.; Zydzik, G. J. Ga_2O_3 Films for Electronic and Optoelectronic Applications. *J. Appl. Phys.* **1995**, *77*, 686−693.

(19) Kauffman, J. F.; Liu, C. S.; Karl, M. W. Surface Recombination Kinetics at the GaAs/Electrolyte Interface via Photoluminescence Efficiency Measurements. *J. Phys. Chem. B* **1998**, *102*, 6766−6773.

(20) Priyantha, W.; Radhakrishnan, G.; Droopad, R.; Passlack, M. In-situ XPS and RHEED Study of Gallium Oxide on GaAs Deposition by Molecular Beam Epitaxy. *J. Cryst. Growth* **2011**, *323*, 103−106.

(21) Wilmsen, C. W.; Kirchner, P. D.; Woodall, J. M. Effects of N_2, O_2, and H_2O on GaAs Passivated by Photowashing or Coating with $Na_2S{\cdot}9H_2O$. *J. Appl. Phys.* **1988**, *64*, 3287−3289.

(22) Choi, K. J.; Moon, J. K.; Park, M.; Kim, H. C.; Lee, J. L. Effects of Photowashing Treatment on Gate Leakage Current of GaAs Metal-Semiconductor Field-Effect Transistors. *Jpn. J. Appl. Phys.* **2002**, *41*, 2894−2899.

(23) Matsumoto, Y.; Yoshikawa, T.; Sato, E. Dependence of the Band Bending of the Oxide Semiconductors on pH. *J. Electrochem. Soc.* **1989**, *136*, 1389−1391.

(24) Yi-Ting, L.; Chien-Shiang, H.; Lee, C.; Jyun-Ming, L.; Chia-Ming, Y.; Liann-Be, C.; Chao-Sung, L. Light-Immune pH Sensor with SiC-Based Electrolyte−Insulator−Semiconductor Structure. *Appl. Phys. Express* **2013**, *6*, 127002.

(25) Gassull, D.; Luber, S. M.; Ulman, A.; Grunze, M.; Tornow, M.; Abstreiter, G.; Tanaka, M. pH Sensitivity of Gallium Arsenide (GaAs) Electrodes Functionalized with Methyl−Mercaptobiphenyl Monolayers. *J. Phys. Chem. C* **2007**, *111*, 12414−12419.

(26) Bavli, D.; Tkachev, M.; Piwonski, H.; Capua, E.; De Albuquerque, I.; Bensimon, D.; Haran, G.; Naaman, R. Detection and Quantification through a Lipid Membrane Using the Molecularly Controlled Semiconductor Resistor. *Langmuir* **2012**, *28*, 1020−1028.

(27) Huang, Y.; Luo, J.; Ivey, D. G. Comparative Study of GaAs Corrosion in H_2SO_4 and $NH_3{\cdot}H_2O$ Solutions by Electrochemical Methods and Surface Analysis. *Mater. Chem. Phys.* **2005**, *93*, 429−442.

(28) Frankenberger, W. T.; Johanson, J. B. Effect of pH on Enzyme Stability in Soils. *Soil Biol. Biochem.* **1982**, *14*, 433−437.

(29) Trivedi, B.; Danforth, W. H. Effect of pH on the Kinetics of Frog Muscle Phosphofructokinase. *J. Biol. Chem.* **1966**, *241*, 4110−4114.

(30) Gilman, A. G. A Protein Binding Assay for Adenosine 3′:5′-Cyclic Monophosphate. *Proc. Natl. Acad. Sci. U. S. A.* **1970**, *67*, 305−312.

DOI: 10.1021/acs.jpcc.6b08844
J. Phys. Chem. C 2016, 120, 26129−26137

(31) Duplan, V.; Miron, Y.; Frost, E.; Grandbois, M.; Dubowski, J. J. Specific Immobilization of Influenza A Virus on GaAs (001) surface. *J. Biomed. Opt.* **2009**, *14*, 054042.
(32) Duplan, V.; Frost, E.; Dubowski, J. J. A Photoluminescence-Based Quantum Semiconductor Biosensor for Rapid in Situ Detection of *Escherichia coli*. *Sens. Actuators, B* **2011**, *160*, 46−51.
(33) Nazemi, E.; Aithal, S.; Hassen, W. M.; Frost, E. H.; Dubowski, J. J. GaAs/AlGaAs Heterostructure Based Photonic Biosensor for Rapid Detection of *Escherichia coli* in Phosphate Buffered Saline Solution. *Sens. Actuators, B* **2015**, *207*, 556−562.
(34) Aziziyan, M. R.; Hassen, W. M.; Morris, D.; Frost, E. H.; Dubowski, J. J. Photonic Biosensor Based on Photocorrosion of GaAs/AlGaAs Quantum Heterostructures for Detection of *Legionella pneumophila*. *Biointerphases* **2016**, *11*, 019301.
(35) Fairley, N. *CasaXPS*, version 2.3.10, 1999−2005.
(36) Bellamy, L. J. *The Infrared Spectra of Complex Molecules*, 3rd ed.; Springer: Netherlands, 1975.
(37) Thompson, W. R.; Cai, M.; Ho, M.; Pemberton, J. E. Hydrolysis and Condensation of Self-Assembled Monolayers of (3-Mercaptopropyl)trimethoxysilane on Ag and Au Surfaces. *Langmuir* **1997**, *13*, 2291−2302.
(38) Kyoung Jin, C.; Jae Kyoung, M.; Min, P.; Haechon, K.; Jong-Lam, L. Effects of Photowashing Treatment on Gate Leakage Current of GaAs Metal-Semiconductor Field-Effect Transistors. *Jpn. J. Appl. Phys.* **2002**, *41*, 2894−2899.
(39) Ruberto, M. N.; Zhang, X.; Scarmozzino, R.; Willner, A. E.; Podlesnik, D. V.; Osgood, R. M. The Laser-Controlled Micrometer-Scale Photoelectrochemical Etching of III−V Semiconductors. *J. Electrochem. Soc.* **1991**, *138*, 1174−1185.
(40) Passlack, M.; Hong, M.; Mannaerts, J. P.; Kwo, J. R.; Tu, L. W. Recombination Velocity at Oxide−GaAs Interfaces Fabricated by in Situ Molecular Beam Epitaxy. *Appl. Phys. Lett.* **1996**, *68*, 3605−3607.
(41) Dubowski, J. J.; Voznyy, O.; Marshall, G. M. Molecular Self-Assembly and Passivation of GaAs (001) with Alkanethiol Monolayers: A View towards Bio-functionalization. *Appl. Surf. Sci.* **2010**, *256*, 5714−5721.
(42) Ding, X.; Moumanis, K.; Dubowski, J. J.; Tay, L.; Rowell, N. L. Fourier-Transform Infrared and Photoluminescence Spectroscopies of Self-Assembled Monolayers of Long-Chain Thiols on (001) GaAs. *J. Appl. Phys.* **2006**, *99*, 054701.
(43) Arudra, P.; Nguiffo-Podie, Y.; Frost, E.; Dubowski, J. J. Decomposition of Thimerosal and Dynamics of Thiosalicylic Acid Attachment on GaAs(001) Surface Observed with in Situ Photoluminescence. *J. Phys. Chem. C* **2010**, *114*, 13657−13662.
(44) Marshall, G. M.; Lopinski, G. P.; Bensebaa, F.; Dubowski, J. J. Electro-Optic Investigation of the Surface Trapping Efficiency in n-Alkanethiol SAM Passivated GaAs(001). *Nanotechnology* **2011**, *22*, 235704.
(45) Hou, T.; Greenlief, C. M.; Keller, S. W.; Nelen, L.; Kauffman, J. F. Passivation of GaAs(100) with an Adhesion Promoting Self-Assembled Monolayer. *Chem. Mater.* **1997**, *9*, 3181−3186.
(46) Aithal, S.; Liu, N.; Dubowski, J. J. Photocorrosion Metrology of Photoluminescence Emitting GaAs/AlGaAs Heterostructures. *J. Phys. D: Appl. Phys.* In press.
(47) Sutter, E. M. M.; Le Gall, M.; Debiemme-Chouvy, C. Behavior of p-Type GaAs in an Aerated Boric Acid Solution at the Open-Circuit Potential. Influence of the Presence of Co(II) Ions. *J. Phys. Chem. B* **2001**, *105*, 4840−4845.
(48) Downs, A. J. *Chemistry of Aluminium, Gallium, Indium and Thallium*, 1st ed.; Springer: Netherlands, 1993.
(49) Cypryk, M.; Apeloig, Y. Mechanism of the Acid-Catalyzed Si−O Bond Cleavage in Siloxanes and Siloxanols. A Theoretical Study. *Organometallics* **2002**, *21*, 2165−2175.
(50) Wilczek, L.; Chojnowski, J. Studies of Siloxane-acid Model System: Hexamethyldisiloxane-Trifluoroacetic Acid. *Makromol. Chem.* **1983**, *184*, 77−90.
(51) Hurd, D. T.; Osthoff, R. C.; Corrin, M. L. The Mechanism of the Base-Catalyzed Rearrangement of Organopolysiloxanes[1]. *J. Am. Chem. Soc.* **1954**, *76*, 249−252.
(52) Alam, A. U.; Howlader, M. M. R.; Deen, M. J. Oxygen Plasma and Humidity Dependent Surface Analysis of Silicon, Silicon Dioxide and Glass for Direct Wafer Bonding. *ECS J. Solid State Sci. Technol.* **2013**, *2*, P515−P523.

DOI: 10.1021/acs.jpcc.6b08844
J. Phys. Chem. C 2016, 120, 26129−26137